applied sciences

MDPI

Article

Modified Structures for Hybrid Active Sound Quality Control System Disturbed by Gaussian Random Noise †

Shanjun Li, Guoyong Jin *, Xiaobo Li and Tiangui Ye

College of Power and Energy Engineering, Harbin Engineering University, Harbin 150001, China; lishanjun98@163.com (S.L.); lixiaobo5014@gmail.com (X.L.); yetiangui@126.com (T.Y.)

* Correspondence: guoyongjin@hrbeu.edu.cn

† This paper is an extended version of paper published in the 48th International Congress and Exhibiton on Noise Control Engineering, Madrid, Spain, 16–19 June 2019.

Received: 3 December 2019; Accepted: 8 January 2020; Published: 10 January 2020

check for updates

Abstract: A hybrid active sound quality control system, in which a hybrid feedforward and feedback structure is applied, can not only be used in cases where the line-spectrum noise is obtained easily with reference sensors, but it can also improve the comfortability of noise and eliminate unexpected Gaussian random noise. However, the traditional structure for a hybrid active sound quality control system, whereby a reference signal in the feedback control structure is synthesized by the output signals of the feedforward control filter, feedback control filter, and line-spectrum noise cancellation control filter, introduces couplings of the three control filters. To remove the coupling interactions of the feedforward and feedback control structures and to reduce the complexity of the control system, two modified structures with less computational complexity or a smaller increase in computation are investigated in this paper. The first one involves a simplified structure in which the reference signal in the feedback control structure is replaced by the summation of the residual error signal and the output signal of the line-spectrum noise cancellation control filter, and the second one is a modified structure which integrates the output signals of the feedback control filter and the line-spectrum noise cancellation control filter for the reference signal in the feedback control structure. Numerical simulations are carried out to show the performance of the modified structures. The results illustrate that the two modified structures have the ability to cancel Gaussian random noise and to reduce or enhance the amplitude of line-spectrum noise to promote sound quality. Moreover, a simplified structure with a new leaky filtered-x least mean square (FxLMS) algorithm is proposed to upgrade the noise reduction performance and elevate stability in the feedback control structure. The effectiveness of the proposed algorithm also is proven by the simulation results.

Keywords: hybrid active sound quality control; line-spectrum noise; gaussian random noise

1. Introduction

Active noise control (ANC) technology is mainly applied to reduce the low-frequency noise at points or zones inside a sound field, such as the area near human ears [1–3]. This technology introduces a controllable secondary sound field that is related to the primary sound field to reduce the sound pressure levels at the controlled points and zones [4]. In other words, the primary noise can be cancelled by the introduction of the secondary sound source, which generates a secondary sound with the opposite phase and the same amplitude as the primary sound in the ANC system [5,6]. However, it is needed to attenuate or enhance the sound pressure levels of certain frequency points or frequency bands to satisfy the requirements of acoustic comfortability in some situations.

To achieve the abovementioned goal, Kuo et al. put forward the adaptive active sound quality control algorithm to shape the residual noise [7]. It was developed on the basis of an adaptive noise equalizer (ANE) in which the pseudo-error noise was minimized instead of the residual noise to update the weight coefficient of the control filter [8–10]. Furthermore, there is a gain factor that one can attenuate, retain, and amplify noise to improve comfortability by setting up an appropriate gain factor value in the adaptive noise equalizer structure. One can combine the ANE structure with different adaptive control algorithms to achieve the control goal of sound quality [11]. For example, a post-masking least mean square (LMS) algorithm was presented to achieve effective sound quality control aimed at vehicle interior noise [12]. A broadband self-tuning ANE system utilizing the filtered-x least mean square (FxLMS) algorithm was researched in Reference [13]. A novel adaptive FxLMS control scheme with better performance of convergence was depicted to pursue sound quality control of sinusoidal noise [14]. It is noted that these control algorithms or control systems used only the feedforward control structure.

The adaptive feedforward control structure is widely applied to ANC systems when a reference signal can be obtained effectively by using reference sensors [15]. However, if there is no suitable position to arrange the reference sensors, the causality and correlation requirement may not be satisfied such that the noise cannot be controlled validly by the feedforward structure [16]. Unlike the feedforward control system, the feedback ANC system does not need a reference sensor to acquire the primary noise information, and the reference signal is the summation of the error signal and the control filter output signal filtered by the estimated model of the secondary path [17,18]. The feedback ANC system is also applied to some actual cases in which the primary noise cannot be detected conveniently and the reference signal is not obtained cost-effectively owing to the existence of many noise sources [19]. Additionally, a simplified feedback ANC system was developed in Reference [19]. The simplified feedback ANC system could decrease the computational load, but the numerical stability became weak in this system. The leaky FxLMS algorithm with a leakage factor was applied to strengthen the numerical stability in the simplified feedback ANC system [19].

Considering that the feedforward and feedback structures have their respective advantages, hybrid structures were developed to reduce correlated noise and eliminate uncorrelated narrowband noise [20–23]. A decoupled hybrid algorithm was proposed by Wu et al. to elevate the performance of the traditional hybrid control algorithm [15]. However, the above-mentioned hybrid control algorithm cannot carry out sound quality control. A traditional hybrid sound quality control algorithm was developed to control the sound quality of line-spectrum noise and reduce the broadband disturbance [10]. The traditional hybrid sound quality control algorithm includes a feedforward structure, a feedback structure, and a line-spectrum noise cancellation control structure. The reference signal in the feedback structure is synthesized by three different signals: the residual error signal, the output signal of the line-spectrum noise cancellation control filter, and the total output signal filtered by the estimated model of the secondary path [15]. It is obvious that the reference signal in the feedback structure depends on the output signals of the three control structures. The residual error signal is also related to the output signals of the three control structures. Therefore, among the three control filters, coupling actions exist that can deteriorate the performance of the whole control system, such as the convergence speed.

To decrease the coupling effect of the whole control system and reduce the complexity of the control structure based on the traditional structure of a hybrid sound quality control system, two modified structures for hybrid sound quality control systems are constructed. The two modified structures can not only control the sound quality of the line-spectrum noise, but they can also cancel Gaussian random disturbance at the error sensors. The first one is a simplified structure that removes the output signal of the feedforward control filter from the combination of the reference signal in the feedback control structure [15]. The reference signal of the feedback control structure is replaced by the summation of the residual error signal and the output signal of the line-spectrum noise cancellation control filter. The second one is a modified structure that integrates the output signals of the feedback control filter and the line-spectrum noise cancellation control filter for the reference input signal in the feedback control structure. Unlike Reference [10], the coupling effects of the three controllers are researched, and the computational complexities of the three hybrid structures are presented. The two modified structures, as two alternate structures of the traditional hybrid structure, can alleviate the coupling effect and intuitively decrease the complexity of structure. Furthermore, in order to improve the performance of the leaky FxLMS algorithm in the simplified feedback ANC system, a simplified structure with a new leaky FxLMS algorithm is proposed to upgrade the noise reduction and elevate stability in the feedback control structure.

2. Traditional Structure for Hybrid Active Sound Quality Control System

Figure 1 shows a schematic diagram of the traditional structure for a hybrid active sound quality control system proposed by Reference [10]. It combines the traditional hybrid structure in Reference [15] and active line-spectrum noise control of sound quality. It also introduces the gain factor β and line-spectrum noise cancellation control structure. This traditional structure includes three parts, the feedforward control structure, the feedback control structure, and the line-spectrum noise cancellation control structure, which correspond to the green rectangle solid-line box, the red rectangle dotted-line box, and the blue rectangle dotted/dashed-line box, respectively, in Figure 1.

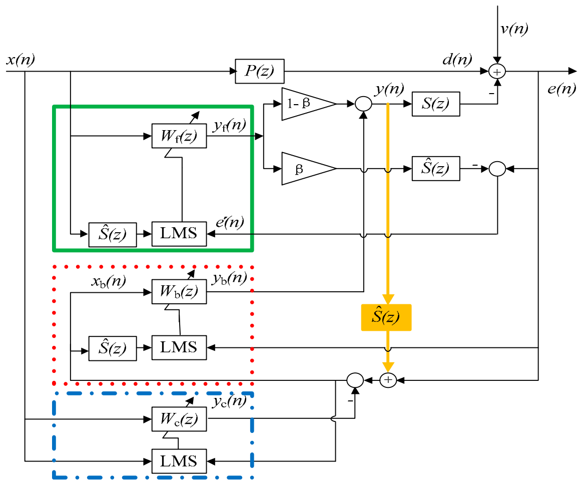

Figure 1. Schematic diagram of the traditional structure for hybrid active sound quality control system.

In the feedforward control structure, the reference signal $x(n)$ can be obtained by a reference sensor. The feedforward controller generates the secondary signal $y_f(n)$ to cancel the desired signal $d(n)$ via the gain adjustment and the secondary path $S(z)$. The desired signal $d(n)$ is the reference signal $x(n)$ via the primary path $P(z)$. The pseudo-error signal $e'(n)$ is the summation of the residual error signal $e(n)$ and the β times secondary signal filtered by the estimated model of the secondary path $\hat{S}(z)$; it can be used to participate in the iteration process of the weight coefficient for the control filter $W_f(z)$ that is expressed as a weight coefficient vector of length M, i.e., $\boldsymbol{w}_f(n) = [w_f(n), w_f(n-1), w_f(n-2), \cdots, w_f(n-M+1)]^T$. In addition, the residual error signal $e(n)$ contains the Gaussian random signal $v(n)$.

The feedback control structure has the reference signal $x_b(n)$ and the control filter $W_b(z)$, which is regarded as a weight coefficient vector of length N. In the feedback control structure, the reference signal is the consolidation of the output signal $y_c(n)$ in the line-spectrum noise cancellation control structure, the residual error signal $e(n)$ and the total output signal $y(n)$ of the hybrid structure filtered by the estimated model of the secondary path $\hat{S}(z)$. The secondary signal $y_b(n)$ is applied to alleviate the Gaussian random disturbance at the error sensor.

The line-spectrum noise cancellation control structure uses the LMS algorithm, but the FxLMS algorithm is applied to the feedforward control structure and feedback control structure. In the line-spectrum noise cancellation control structure, the reference input signal $x_b(n)$ is utilized to participate in the iteration process of the weight coefficient for control filter $W_c(z)$, which is considered as a weight coefficient vector of length L. The output signal $y_c(n)$ generated by control filter $W_c(z)$ is used to eliminate the line-spectrum noise that exists in residual error signal $e(n)$. The acquirement of the reference signal $x(n)$ in the line-spectrum noise cancellation control structure is the same as that in the feedforward control structure.

To analyze the coupling effects of the three control structures, some formulas are derived below. By utilizing the Z-transforms, in the feedforward control structure, the residual error signal is described as

$$E(z) = D(z) + V(z) - Y(z)S(z), \tag{1}$$

where $Y(z)$ is the total output signal of hybrid structure.

$$Y(z) = (1-\beta)Y_f(z) + Y_b(z), \tag{2}$$

where β is the gain factor which can be selected on the basis of the control target of sound quality, $Y_f(z)$ is the output signal of the feedforward control structure, and $Y_b(z)$ is the output signal of the feedback control structure.

$$Y_f(z) = X(z)W_f(z), \tag{3}$$

$$Y_b(z) = X_b(z)W_b(z), \tag{4}$$

where $W_f(z)$ is the feedforward control filter, and $W_b(z)$ is the feedback control filter, while $X(z)$ is the reference input signal in the feedforward and line-spectrum noise cancellation control structures, and $X_b(z)$ is the reference input signal of the feedback control structure.

$$X_b(z) = E(z) + Y(z)\hat{S}(z) - Y_c(z), \tag{5}$$

where $Y_c(z)$ is the output signal of the line-spectrum noise cancellation control structure, which can be obtained by

$$Y_c(z) = X(z)W_c(z), \tag{6}$$

where $W_c(z)$ is the line-spectrum noise cancellation control filter.

Upon substituting Equations (2)–(4) and (6) into Equation (5), and further reorganizing it, one gets

$$X_b(z) = \frac{E(z) + [(1-\beta)\hat{S}(z)W_f(z) - W_c(z)]X(z)}{1-\hat{S}(z)W_b(z)}. \tag{7}$$

Substituting Equations (2)–(4) and (7) into Equation (1) gives

$$E(z) = D(z) + V(z) - S(z)\{(1-\beta)X(z)W_f(z) + \frac{E(z) + [(1-\beta)\hat{S}(z)W_f(z) - W_c(z)]X(z)}{1-\hat{S}(z)W_b(z)}W_b(z)\}. \tag{8}$$

Upon rearranging Equation (8), after further derivation, one obtains

$$E(z) = \frac{1-\hat{S}(z)W_b(z)}{1+W_b(z)[S(z)-\hat{S}(z)]}[D(z)+V(z)] - \frac{(1-\beta)W_f(z) - W_c(z)W_b(z)}{1+W_b(z)[S(z)-\hat{S}(z)]}S(z)X(z), \tag{9}$$

where $D(z) = X(z)P(z)$, and $P(z)$ is the main path from the reference sensor to error sensor.

Then, the residual error signal of the traditional structure for the hybrid active sound quality control system is yielded by

$$E(z) = \frac{1-\hat{S}(z)W_b(z)}{1+W_b(z)[S(z)-\hat{S}(z)]}V(z) + \frac{[1-\hat{S}(z)W_b(z)]P(z) - [(1-\beta)W_f(z) - W_c(z)W_b(z)]S(z)}{1+W_b(z)[S(z)-\hat{S}(z)]}X(z). \tag{10}$$

Assuming that $S(z) = \hat{S}(z)$ is applicable to Equation (10), the residual error signal $E(z)$ can be written as

$$E(z) = [1 - S(z)W_b(z)]V(z) + \Big\{[1 - S(z)W_b(z)]P(z) - [(1-\beta)W_f(z) - W_c(z)W_b(z)]S(z)\Big\}X(z). \quad (11)$$

It is clear in Equation (11) that there are coupling effects among the feedforward control filter $W_f(z)$, the feedback control filter $W_b(z)$, and the line-spectrum noise cancellation control filter $W_c(z)$. Considering the gain factor β as equal to zero, the sound quality control system becomes a common ANC system. In an ANC system, the term $[1 - S(z)W_b(z)]P(z) - [W_f(z) - W_c(z)W_b(z)]S(z)$ is nearly zero when the desired signal $d(n)$ is offset. Then, one has

$$W_f(z) = \frac{[1 - S(z)W_b(z)]P(z)}{S(z)} + W_c(z)W_b(z) = \frac{P(z)}{S(z)/[1 - S(z)W_b(z)]} + W_c(z)W_b(z). \quad (12)$$

Because the line-spectrum noise in the residual error signal is eliminated, the line-spectrum noise cancellation control filter $W_c(z)$ approaches zero. Therefore, the coupling effect of the control system is presented as the influence of the feedback control filter on the feedforward control filter, which might result in the divergence of the feedforward control filter $W_f(z)$ during the iteration of the weight coefficient in the feedback control filter $W_b(z)$. Moreover, the coupling effect of the control system is such that the convergence of $W_f(z)$ is subject to the updates of $W_b(z)$ and $W_c(z)$ when the gain factor is not equal to zero. It is observed in Equation (5) that the coupling effect exists in this control system because the output signals of the three control structures participate in the synthesis of the reference signal.

3. Modified Structures for Hybrid Active Sound Quality Control System

3.1. The Simplified Structure for a Hybrid Active Sound Quality Control System with a New Leaky FxLMS Algorithm

A modified structure, later called the simplified structure, is proposed on the basis of the traditional structure for hybrid active sound quality control. This simplified structure can reduce the coupling effect of the control filters and decrease the computational complexity of the control structure. Figure 2 shows a schematic diagram of the simplified structure for a hybrid active sound quality control system. It can be seen from Figure 2 that the simplified structure has a simplification in the feedback control structure compared to the traditional structure. The reference input signal $x_b(n)$ in the feedback control structure is now superseded by the synthesis of the residual error signal $e(n)$ and the output signal $y_c(n)$ of the line-spectrum noise cancellation control filter, i.e.,

$$X_b(z) = E(z) - Y_c(z). \quad (13)$$

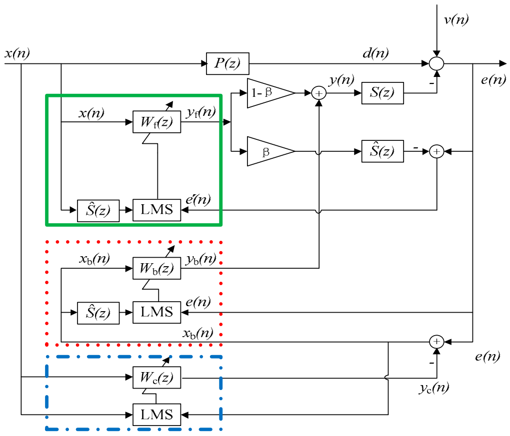

Figure 2. Schematic diagram of the simplified structure for the hybrid active sound quality control system.

From Equation (13), the merit can be seen that the term $\hat{S}(z)Y(z)$ is removed in the reference input signal of the feedback control structure. Therefore, the computational complexity of the control structure is decreased.

Supposing $S(z) = \hat{S}(z)$ and $D(z) = X(z)P(z)$, one can derive the residual error signal by imitating the deduction of Equation (11) and substituting Equation (13) into Equation (5).

$$E(z) = \frac{1}{1 + S(z)W_b(z)}V(z) + \frac{P(z) - [(1-\beta)W_f(z) - W_c(z)W_b(z)]S(z)}{1 + S(z)W_b(z)}X(z). \quad (14)$$

Because the residual error signal changes with the sound quality control goals, the coupling is discussed based on the residual error signal in Equation (14). From Equation (14), it can be seen that there is less coupled correlation between the feedforward and feedback control structure because of the use of the reference signal in Equation (13) when the simplified structure is compared with the traditional structure for the hybrid active sound quality control system. When the control system turns into an ANC system, i.e., the gain factor β is set to zero and $W_c(z)$ approaches zero, it can be shown that the update of the weight coefficient for the feedforward control filter has nothing to do with the feedback control filter. The line-spectrum noise cancellation controller also does not influence the iteration of the feedforward controller. In order to attenuate the broadband disturbance $v(n)$ and the primary signal $x(n)$, the feedback control filter is updated to make the expression $1 + S(z)W_b(z)$ as large as possible. The feedback control filter is also close to $P(z)/S(z)$. Furthermore, when the gain factor is non-zero, the coupling effect between the feedback control structure and feedforward control structure is degraded in comparison with the traditional structure, even if the iterations of control filters $W_c(z)$ and $W_b(z)$ still affect the convergence of $W_f(z)$.

The feedback control structure in Figure 2 is identical to the feedback control structure of an ANC system in Reference [10]. Although the total control system is simplified by removing the term $\hat{S}(z)Y(z)$, several drawbacks exist in the feedback control structure because of the use of the reference signal, as presented in Equation (13). The control filter $W_b(z)$ may produce a large value in some iterations such that the feedback control structure becomes instable. Accordingly, the leaky FxLMS algorithm was applied to the feedback control structure to limit the excessive weight value of the filter $W_b(z)$ [24,25]. The cost function of the abovementioned algorithm is not the minimization of the squared residual error signal, and this cost function can deteriorate the capability of noise reduction.

The filter output is not constrained, and the noise attenuation performance is deteriorated owing to the utilization of the leaky FxLMS algorithm in the feedback control structure [26]. To overcome the weakness and improve the noise attenuation performance, a new leaky FxLMS algorithm with a time-varying leakage factor is used for the feedback control structure on the basis of the anti-Hebbian constraint in Reference [27]. In the time domain, the iteration formula of the feedback control filter becomes

$$w_b(n+1) = \frac{w_b(n) + \mu e(n) x_b(n) \hat{s}(n)}{1 + \mu e(n) v(n)}, \tag{15}$$

where $w_b(n)$ is the weight coefficient for the control filter $W_b(z)$, $\hat{s}(n)$ is the impulse response of the estimated secondary path model $\hat{S}(z)$, and μ is the step size.

If the absolute value of the term $\mu e(n)v(n)$ is less than one, one can obtain

$$w_b(n+1) = w_b(n) + \mu e(n)[x_b(n)\hat{s}(n) + w_b(n)v(n)] + o(\mu^2), \tag{16}$$

where $o(\cdot)$ denotes an operator of the infinitesimal.

Rearranging Equation (16), one yields

$$w_b(n+1) = w_b(n)[1 + \mu e(n)v(n)] + \mu e(n) x_b(n) \hat{s}(n). \tag{17}$$

It is indicated in Equation (17) that the stable leaky factor in the leaky FxLMS algorithm is replaced by the term $e(n)v(n)$. In the new leaky FxLMS algorithm, the term $\mu e(n)v(n)$ is regarded as the constraint to avoid the excessive weight value of feedback control filter.

3.2. The Modified Structure for a Hybrid Active Sound Quality Control Structure

Considering that the use of the leaky FxLMS algorithm in the simplified structure for the hybrid sound quality control system weakens the ability of noise attenuation in the feedback control structure, a modified structure for the hybrid sound quality control system is proposed to solve this problem. A schematic diagram of the modified structure for the hybrid active sound quality control system is shown in Figure 3. Unlike the traditional structure, the reference signal $x_b(n)$ in the feedback control structure is now synthesized by the residual error signal $e(n)$, the output signal $y_c(n)$ in the line-spectrum noise cancellation control structure, and the secondary signal $y_b(n)$ of the feedback control structure filtered by the estimated model of the secondary path $\hat{S}(z)$. By using the Z-transforms, the reference signal in the feedback control structure is described as

$$X_b(z) = E(z) + \hat{S}(z) Y_b(z) - Y_c(z). \tag{18}$$

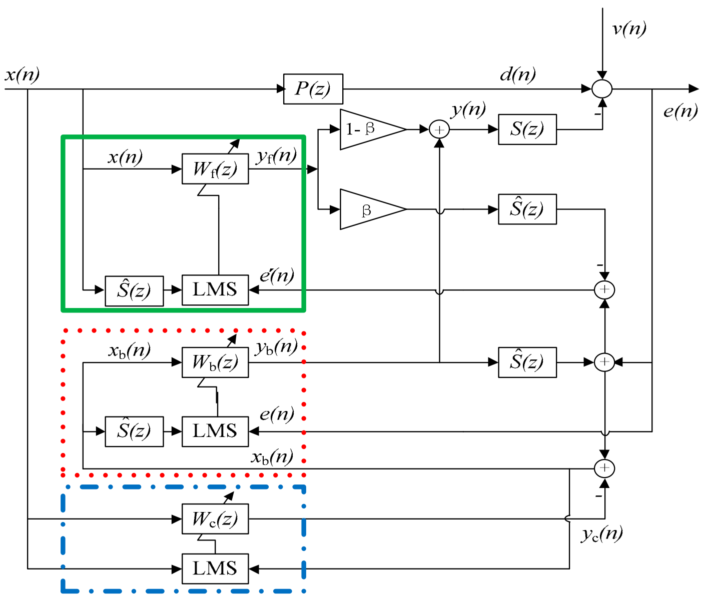

Figure 3. Schematic diagram of the modified structure for the hybrid active sound quality control system.

When $S(z) = \hat{S}(z)$ and $D(z) = X(z)P(z)$ is established, the residual error signal is derived as follows:

$$E(z) = [1 - S(z)W_b(z)]V(z) + \left\{[1 - S(z)W_b(z)][P(z) - (1-\beta)S(z)W_f(z)] + S(z)W_c(z)W_b(z)\right\}X(z). \quad (19)$$

Because the residual error signal varies with the sound quality control goals, the coupling is discussed based on the residual error signal in Equation (19). It is shown clearly in Equation (19) that the feedback and feedforward control filters in this modified structure are decoupled if $W_c(z)$ is small enough. Furthermore, this modified structure has less of a coupling effect because of the use of the reference signal in Equation (18) when this modified structure is compared with the traditional structure for hybrid active sound quality control system. The term $1 - S(z)W_b(z)$ approaches zero to offset the Gaussian random signal $v(n)$. When the gain factor β is equal to zero, the feedforward control filter $W_f(z)$ is equal to $P(z)/S(z)$, and the line-spectrum noise control filter $W_c(z)$ is approximately zero, which can eliminate the desired signal. It can be seen that the desired signal $d(n)$ is reduced by the output signals of the feedforward control filter $W_f(z)$ and feedback control filter $W_b(z)$.

Moreover, it can be seen that the synthesis of the pseudo-error signal in the feedforward control structure is different by comparing Figures 1 and 3. The pseudo-error signal in the feedforward control structure is composed of the residual error signal $e(n)$, the secondary signal $y_b(n)$ filtered by the estimated model of the secondary path $\hat{S}(z)$, and β times the output signal $y_f(n)$ filtered by the estimated model of the secondary path $\hat{S}(z)$. The pseudo-error signal can be described as

$$\begin{aligned} E'(z) &= E(z) + \hat{S}(z)Y_b(z) - \beta\hat{S}(z)Y_f(z) = X_b(z) + Y_c(z) - \beta\hat{S}(z)Y_f(z) \\ &= D(z) + V(z) + [\hat{S}(z) - S(z)]Y_b(z) - S(z)Y_f(z) + \beta[S(z) - \hat{S}(z)]Y_f(z). \end{aligned} \quad (20)$$

If $S(z) = \hat{S}(z)$ is applied to Equation (20), one can obtain

$$E'(z) = D(z) + V(z) - S(z)Y_f(z). \quad (21)$$

The connection between the pseudo-error signal and the reference input signal in the feedback structure is shown in Equation (20). It is obvious in Equation (21) that the production of the pseudo-error signal does not introduce an extra term compared to the traditional structure.

4. Computational Complexity Analysis

The computational complexity is analyzed in view of additions and multiplications [28]. The computational complexities of different structures are shown in Table 1, where M, N, and L are the length of the control filters $W_f(z)$, $W_b(z)$, and $W_c(z)$, respectively. Moreover, H represents the length of the estimated secondary path $\hat{S}(z)$. In Table 1, the "tra structure" is defined as the traditional structure in Reference [10]. The "sim structure" is the simplified structure using the FxLMS algorithm in the feedback control filter. The "tsim structure" represents the simplified structure using the traditional leaky FxLMS algorithm in the feedback control filter [19]. The "nsim structure" expresses the simplified structure using the new leaky FxLMS algorithm in the feedback control filter. Finally, the "mod structure" means the modified structure.

Table 1. Computational complexities of the proposed structures compared to traditional structure.

Structure	Additions	Multiplies	Complexity
tra structure [10]	2(M + N + L) + 4H	2(M + N + L) + 4H + 5	4(M + N + L) + 8H + 5
sim structure	2(M + N + L) + 3H	2(M + N + L) + 3H + 5	4(M + N + L) + 6H + 5
tsim structure [19]	2(M + N + L) + 3H + 1	2(M + L) + 3(H + N) + 6	4(M +L) + 5N + 6H + 7
nsim structure	2(M + N + L) + 3H + 1	2(M + L) + 3(H + N) + 7	4(M + L) + 5N + 6H + 8
mod structure	2(M + N + L) + 5H	2(M + N + L) + 5H + 5	4(M + N + L) + 10H + 5

It is obvious from Table 1 that the "sim structure" has the lowest computational cost in different control structures, and the computational cost of the "mod structure" is slightly increased compared to the "tra structure". The computational complexity of the "mod structure" is only $2H$ more than that of the "tra structure". In the simplified structure, the leaky FxLMS algorithm and new leaky FxLMS algorithm have more computational load than the FxLMS algorithm. The computational load of the "tsim structure" is $N+2$ more than that of the "sim structure". The computational load of the "nsim structure" is $N+3$ more than that of the "sim structure". The computational load of the "nsim structure" is only one more than that of the "tsim structure". Therefore, the simplified structure and the modified structure have better performance than the traditional structure. Meanwhile, the performance of the simplified structure can be improved by the use of the new leaky FxLMS algorithm in the feedback control filter.

On the basis of the digital signal processor TMS320C6748, the computing time of different structures is shown in Table 2, where M, N, and L are 512, and H is 4. The computing time is acquired when the weight coefficients of the control filters are updated one at a time.

Table 2. Computing time of the proposed structures compared to the traditional structure.

Structure	Tra Structure [10]	Sim Structure	Tsim Structure [19]	Nsim Structure	Mod Structure
Time (μs)	15.46	15.44	17.49	17.50	15.48

5. Simulations and Discussion

5.1. Simulation Parameters

The simulation parameters of the two modified structures for the hybrid active sound quality control system were set up to study their performance. The mathematic models of the main path $P(z)$ and the secondary path $S(z)$ were in keeping with Reference [10] for convenience of comparison because the traditional structure was discussed therein.

$$P(z) = 0.0167 + 0.4833z^{-1} + 0.4833z^{-2} + 0.0167z^{-3}. \tag{22}$$

$$S(z) = 0.2037z^{-1} + 0.5926z^{-2} + 0.2037z^{-3}. \tag{23}$$

At the same time, it is presumed that the estimated model of the secondary path $\hat{S}(z)$ was equal to $S(z)$.

In the simulation, two components were contained in the noise signal; the first was the line-spectrum noise $x(n)$, and the second was the Gaussian random noise $v(n)$. The line-spectrum noise $d(n)$ could be acquired by filtering the reference input signal $x(n)$ via $P(z)$. The frequency of the primary noise was 56 Hz, and the amplitude of the signal was 1 Pa. The Gaussian random noise $v(n)$ was set to a bandlimited random noise such that 50 Hz was the center frequency and the bandwidth was 100 Hz. The lengths of the feedforward control filter $W_f(z)$, the feedback control filter $W_b(z)$, and the line-spectrum noise control filter $W_c(z)$ were 512, and the step sizes μ_1, μ_2, and μ_3 were 0.0005, 0.005, and 0.005, respectively. Additionally, the sampling frequency was 10,240 Hz, and the length of the simulation was 4 s.

5.2. Simulation Results and Discussion

Figure 4 presents the converged filter weight coefficients of feedforward control structures and feedback control structures for different hybrid sound quality control systems. The converged filter weight coefficients were calculated when the gain factor was set to 0.5. The "FF structure" expresses the feedforward structure alone, and the "FB structure" represents the feedback structure alone. The "tra structure", "nsim structure", "mod structure", and "sim structure" are defined as in Section 4. The filter weight vectors of the feedforward or feedback structure alone were regarded as the reference filter weight vector $\boldsymbol{w}_r$, and the filter weight vectors of other structures were the comparative filter weight vectors $\boldsymbol{w}$. The discrepancy D was calculated as follows [15]:

$$D = 20 \log_{10} \frac{\|\boldsymbol{w} - \boldsymbol{w}_r\|_2}{\|\boldsymbol{w}_r\|_2}, \tag{24}$$

where $\|\cdot\|_2$ denotes the Euclidean norm.

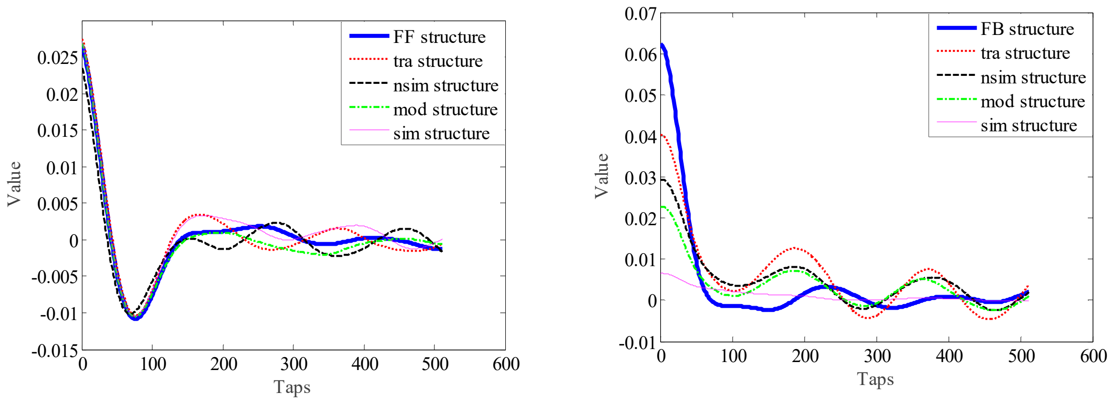

(**a**) (**b**)

Figure 4. Converged filter weight coefficients of (**a**) feedforward control structures and (**b**) feedback control structures for different hybrid sound quality control systems.

It can be seen that the discrepancy can validate the effects of the feedback and line-spectrum noise cancellation control filters on feedforward structure. A smaller discrepancy results in a smaller influence of the feedback and line-spectrum noise cancellation control filters on the feedforward structure. The discrepancy between the "FF structure" and the "tra structure" was −11.4 dB, and that between the "FF structure" and the "nsim structure" was −15.6 dB. Meanwhile, the discrepancy between the "FF structure" and the "sim structure" was −13.1 dB, and that between the "FF structure" and the "mod structure" was −14.7 dB. Furthermore, it should be noted that the two modified hybrid structures had less of a coupling effect compared to the traditional hybrid structure, as depicted in Equations (14) and (19). From Figure 4a, it can also be seen that the two modified hybrid structures had more stable iteration processes in feedforward control filters. At the same time, the discrepancy in Figure 4b was also calculated. The discrepancy between the "FB structure" and the "nsim structure" was −4.8 dB, while that between the "FB structure" and "sim structure" was −1.1 dB. However, the discrepancy between the "FB structure" and "tra structure" was −5.5 dB, and the discrepancy between the "FB structure" and "mod structure" was −3.8 dB. It is indicated that the discrepancy of the modified hybrid structures did not improve owing to the influence of the line-noise cancellation controller when the gain factor was equal to 0.5. As a result, under the synthetic effect of the feedforward and feedback control filters, the three hybrid structures had the same noise reduction.

The objective assessments of the different structures are shown by the noise attenuation as a function of frequency [29]. The gain factor can determine the degree of noise control. When the gain factor is zero, the sound quality control systems become ANC systems where the noise to be controlled is minimized. Meanwhile, the noise to be controlled can be reduced, retained, and amplified when the gain factor is not equal to zero. Therefore, only two gain factors of 0 and 0.5 were selected to validate the performances of the different structures. In addition, the leakage factor of 0.8 was selected in the leaky FxLMS algorithm for the simplified structure because this case had better performance.

Figure 5 shows the spectra of noise attenuation in different structures when the ANC was turned on and off. "ANCoff" represents that the ANC was turned off, whereas "ANCon" represents that the ANC was turned on. Figure 6 depicts the power spectrum densities (PSDs) of noise attenuation in different structures when the ANC was off and on. The gain factor was equal to zero in Figures 5 and 6. It is shown that the two modified algorithms could not only offset the line-spectrum noise to achieve the control goal for sound quality, but they could also attenuate the Gaussian random noise. The total sound pressure levels between 10 Hz and 100 Hz were calculated as follows [30]:

$$SPL = 20\log_{10}(\frac{p}{p_{ref}}), \tag{25}$$

where p denotes the sound pressure, $p_{ref} = 2 \times 10^{-5}$Pa is the reference sound pressure in the air, and SPL denotes the sound pressure level.

$$T\_SPL = 10\log_{10}(\sum_{i=i_{low}}^{i_{high}} 10^{SPL_i/10}), \tag{26}$$

where T_SPL denotes the total sound pressure level.

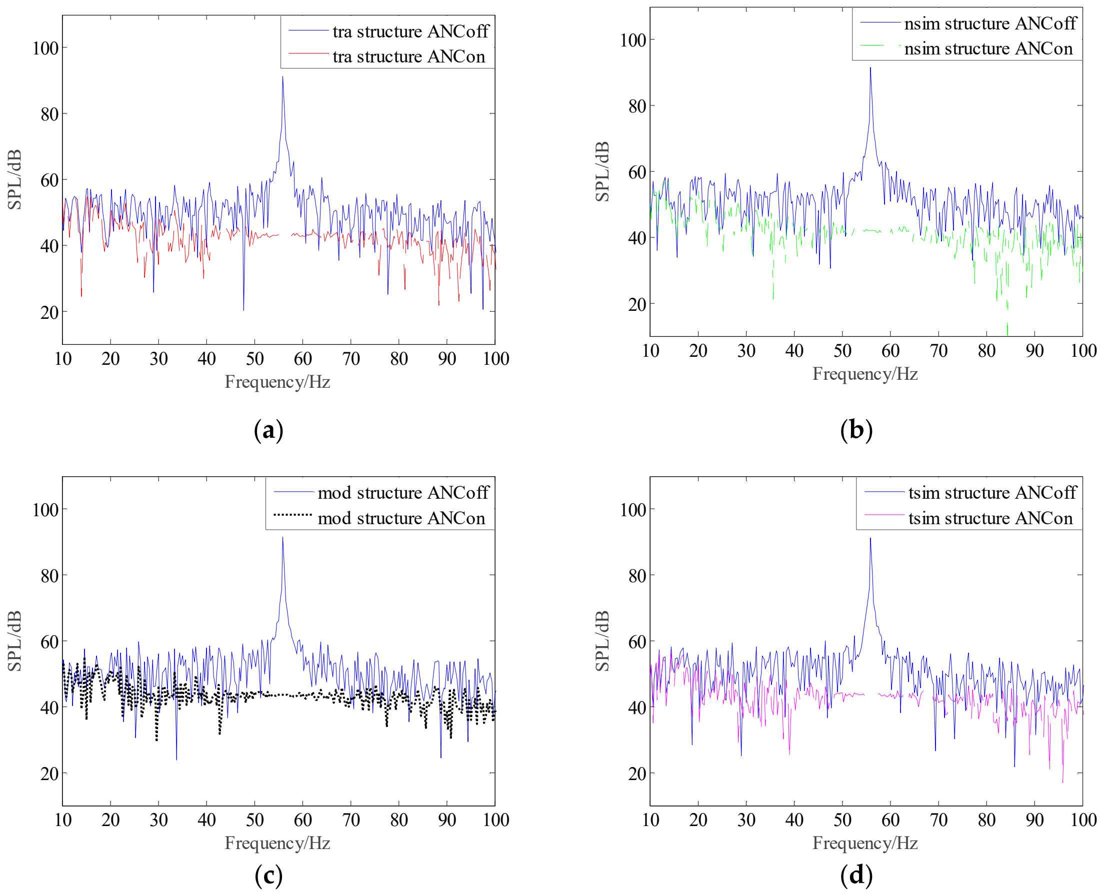

Figure 5. Spectra of noise attenuation in different structures (β = 0): (**a**) traditional hybrid structure; (**b**) simplified hybrid structure using new leaky filtered-x least mean square (FxLMS) algorithm in the feedback controller; (**c**) modified hybrid structure; (**d**) simplified hybrid structure using leaky FxLMS algorithm in the feedback controller (γ = 0.8).

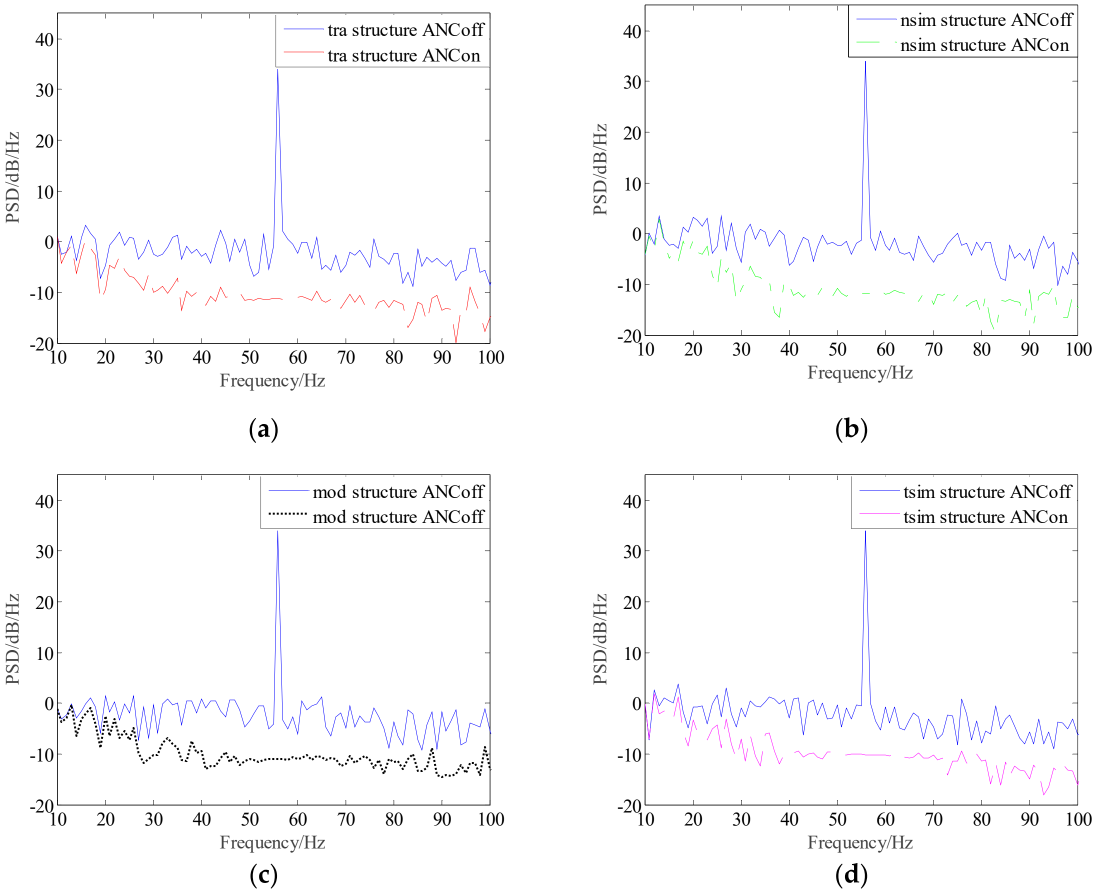

Figure 6. Power spectrum densities (PSDs) of noise attenuation in different structures (β = 0): (**a**) traditional hybrid structure; (**b**) simplified hybrid structure using new leaky FxLMS algorithm in the feedback controller; (**c**) modified hybrid structure; (**d**) simplified hybrid structure using leaky FxLMS algorithm in the feedback controller (γ = 0.8).

The total sound pressure levels of different structures are shown in Table 3. The SPL is defined as the sound pressure level. The total sound pressure level of the modified structure was 69.5 dB when that of the primary noise was 92.1 dB. The total sound pressure level of the traditional structure was close to that of the modified structure. The modified structure not only had a more stable iteration process, but it also had basically the same noise reduction as the traditional structure. This also validated that the beneficial influence of decoupling was balanced with computational complexity because the iteration process of the line-spectrum noise cancellation filter still occurred in practice. The total sound pressure levels of the simplified structures were slightly higher than those of the traditional structure, owing to the use of leaky class FxLMS algorithms in the feedback controllers. Although the computational complexities of the simplified structure using leaky class FxLMS algorithms were less increased, their iteration processes of control filters were more stable. Therefore, it can be obtained that the simplified structures had the approximate ability of noise reduction compared with the traditional structure, because the simplified structures had better performance in terms of stability.

Table 3. Noise reductions of the different structures (β = 0).

Structure	ANCoff	Tra Structure [10]	Tsim Structure [19]	Nsim Structure	Mod Structure
SPL (dB)	92.1	69.4	70.1	70.0	69.5

Furthermore, it can be noted that only the harmonic noise signal was utilized to validate the algorithm performance. The reference input signal with multiple frequencies could be controlled by configuring multiple feedforward sound quality controllers in parallel.

The spectra of noise attenuation in different structures are shown in Figure 7 when the gain factor was 0.5. The noise reductions were measured when the ANC system was turned off and on. The total sound pressure levels of different structures are also calculated in Table 4. Figure 8 illustrates the power spectrum densities (PSDs) of noise attenuation in different structures when the gain factor was equal to 0.5. The primary noise signal included the line-spectrum noise signal and the Gaussian random noise signal. From Figures 7 and 8, it can be seen that the two modified structures for the hybrid active sound quality control systems could not only control sound quality of line-spectrum noise by decreasing the noise amplitude, but they could also reduce the Gaussian random noise. The different gain factors could also be selected to retain and amplify the noise amplitude to achieve the goal of control sound quality. Meanwhile, the noise reductions of the two modified structures were equivalent to that of the traditional structure because of the influence of the gain factor on the coupling effect. The noise reductions in the different structures were about 6.0 dB between 10 Hz and 100 Hz, and the simulation results were in accordance with the theoretical calculations in Reference [10].

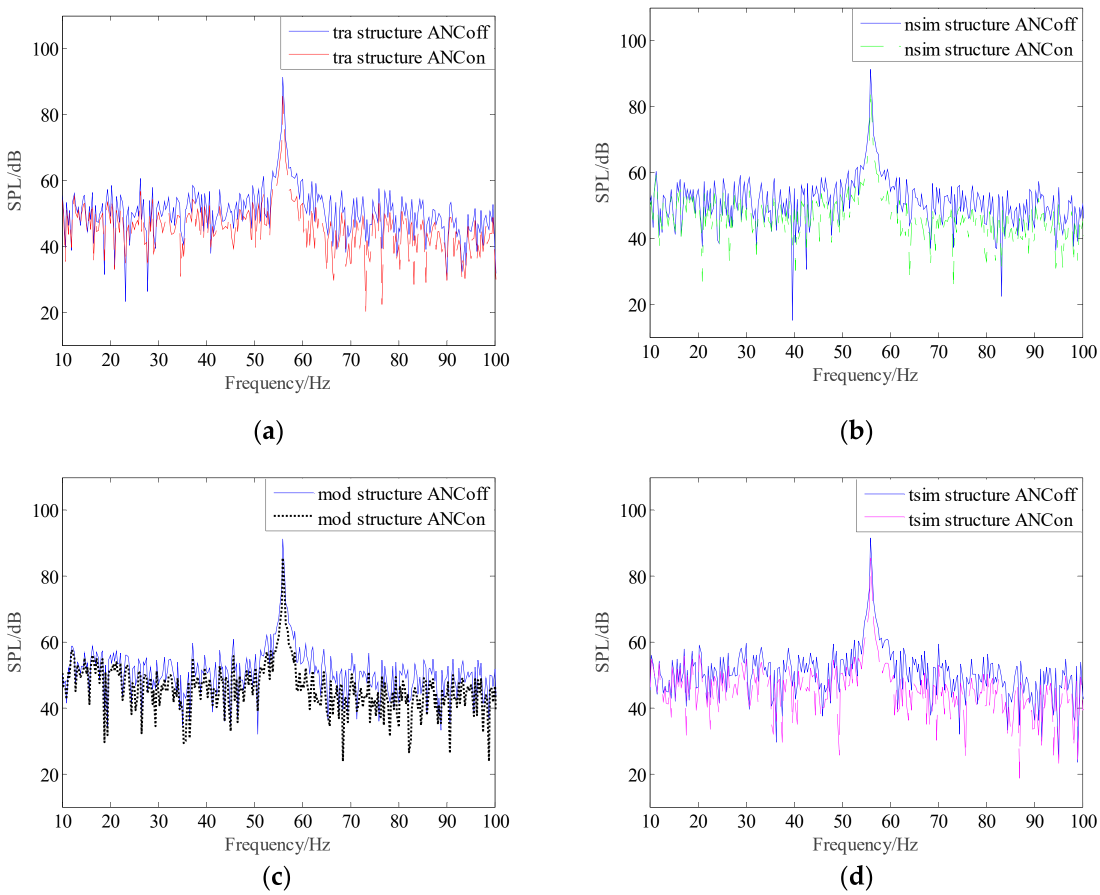

Figure 7. Spectra of noise attenuation in different structures (β = 0.5): (**a**) traditional hybrid structure; (**b**) simplified hybrid structure using new leaky FxLMS algorithm in the feedback controller; (**c**) modified hybrid structure; (**d**) simplified hybrid structure using leaky FxLMS algorithm in the feedback controller (γ = 0.8).

Table 4. Noise reductions of the different structures (β = 0.5).

Structure	ANCoff	Tra Structure [10]	Tsim Structure [19]	Nsim Structure	Mod Structure
SPL (dB)	92.1	86.2	86.2	86.1	86.2

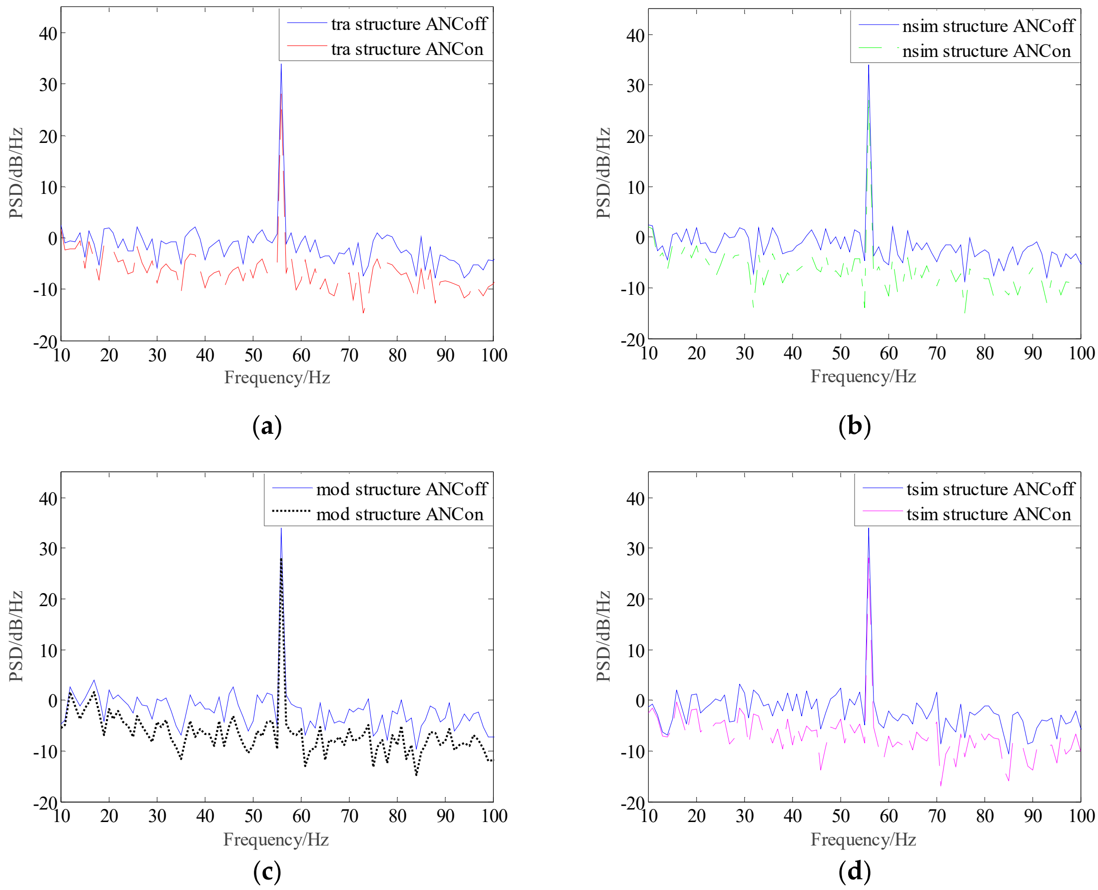

Figure 8. PSDs of noise attenuation in different structures β = 0.5): (**a**) traditional hybrid structure; (**b**) simplified hybrid structure using new leaky FxLMS algorithm in the feedback controller; (**c**) modified hybrid structure; (**d**) simplified hybrid structure using new leaky FxLMS algorithm in the feedback controller (γ = 0.8).

Figure 9 describes the waveforms of output signals for feedback control filters using different algorithms when the step size of the feedback control filter was 0.005 and the gain factor was 0.5. Figure 9a indicates the waveforms of output signals for the feedback control filters using the FxLMS algorithm, the new leaky FxLMS algorithm, and the leaky FxLMS algorithms with different leakage factors. It can be seen that the output signals for the feedback control filters using the leaky class FxLMS algorithms were more stable compared to the one using the FxLMS algorithm because some iterations of the feedback control filter were unstable. Meanwhile, it is indicated in Figure 9b–d that the feedback control filter with the new leaky FxLMS algorithm had better constraint performance, avoiding the excessive output signal of the feedback control filter. However, the output signal of the feedback control filter with the new leaky FxLMS algorithm fluctuated remarkably because the constraint term was updated in real time, as presented in Equation (17). Furthermore, the fluctuation slightly enabled the amplitude of the output signal to maintain a high level, which resulted in a higher noise reduction compared to the leaky FxLMS algorithm with a constant leakage factor.

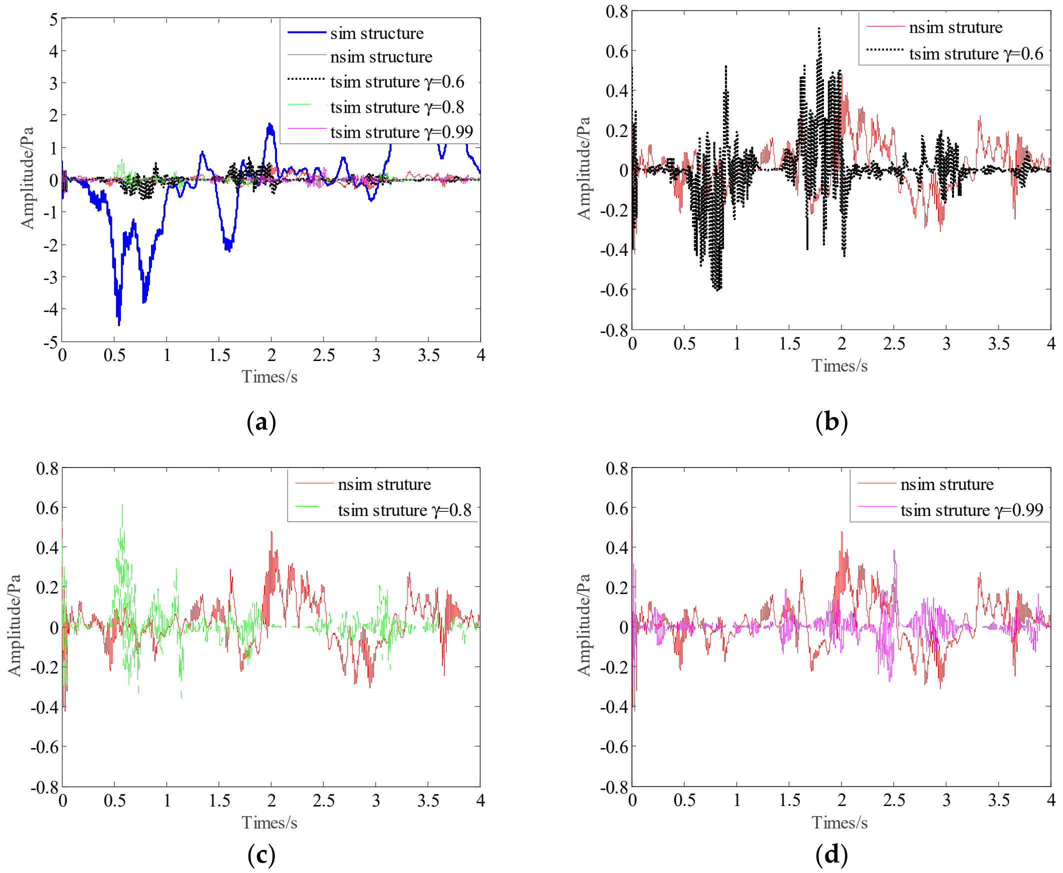

Figure 9. Waveforms of the output signals for the feedback control filter in the simplified structure using the new leaky FxLMS algorithm, and (**a**) using the FxLMS algorithm, (**b**) using the leaky FxLMS algorithm ($\gamma = 0.6$), (**c**) using the leaky FxLMS algorithm($\gamma = 0.8$), and (**d**) using the leaky FxLMS algorithm ($\gamma = 0.99$).

It is shown in Figures 10 and 11 that noise reductions of the new leaky FxLMS algorithm and the leaky FxLMS algorithm with a constant leakage factor ($\gamma = 0.8$) were correlated when the gain factor was set to zero. The noise reductions in different frequency ranges are calculated in Table 5. The noise reduction of the new leaky FxLMS algorithm between 50 Hz and 65 Hz was 33.3 dB, while that of the leaky FxLMS algorithm with a constant leakage factor ($\gamma = 0.8$) was 31.7 dB. The noise reduction of the new leaky FxLMS algorithm between 40 Hz and 80 Hz was 29.5 dB, while that of the leaky FxLMS algorithm with a constant leakage factor ($\gamma = 0.8$) was 27.8 dB. The noise reduction of the new leaky FxLMS algorithm between 20 Hz and 100 Hz was 24.7 dB, while that of the leaky FxLMS algorithm with a constant leakage factor ($\gamma = 0.8$) was 24.6 dB. The noise reduction of the new leaky FxLMS algorithm between 10 Hz and 100 Hz was 22.1 dB, while that of the leaky FxLMS algorithm with a constant leakage factor ($\gamma = 0.8$) was 22.0 dB. It can be observed easily that the noise reductions of the two leaky FxLMS algorithms diminished with increasing bandwidth, and the new leaky FxLMS algorithm had a higher noise reduction. In other words, the leaky FxLMS algorithm had the better performance of noise reduction in a narrow relative frequency band where the center frequency for sound quality control was contained. In addition, upon increasing the length of the control filter and the sampling frequency, the two leaky FxLMS algorithms had a wider frequency band for noise reduction. The step size of the leakage term in the new leaky FxLMS algorithm could be distinguished from that of the total control algorithm. The value range of the step size in the leakage term could be from 0.00005 to 0.05.

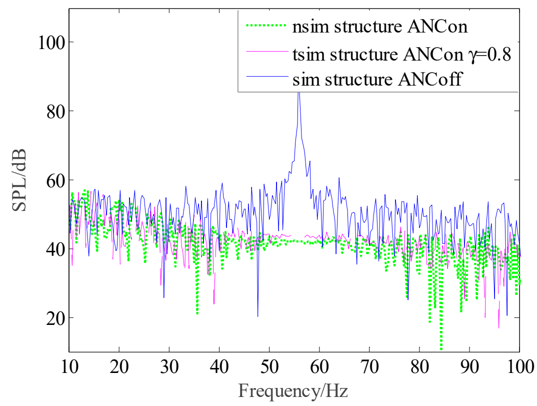

Figure 10. Spectra of noise reductions in simplified structure using the new leaky FxLMS algorithm and the leaky FxLMS algorithm (β = 0).

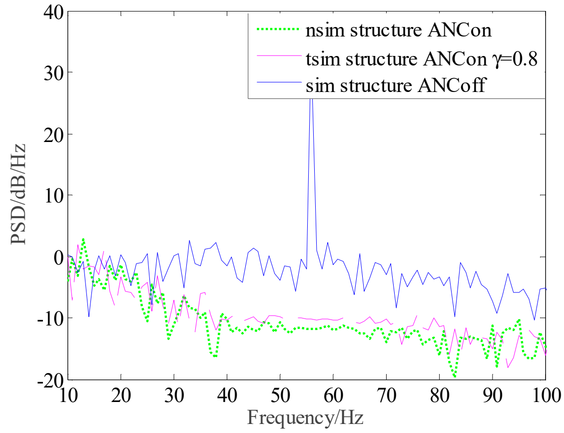

Figure 11. PSDs of noise reductions in simplified structure using the new leaky FxLMS algorithm and the leaky FxLMS algorithm (β = 0).

Table 5. Noise reductions of simplified structure using the new leaky filtered-x least mean square (FxLMS) algorithm and the leaky FxLMS algorithm (β = 0) in the different frequency ranges.

Structure	Noise Reduction Between 10 Hz and 100 Hz (dB)	Noise Reduction Between 20 Hz and 100 Hz (dB)	Noise Reduction Between 40 Hz and 80 Hz (dB)	Noise Reduction Between 50 Hz and 65 Hz (dB)
tsim structure [19]	22.1	24.7	29.5	33.3
nsim structure	22.0	24.6	27.8	31.7

6. Conclusions

In this paper, two modified structures for hybrid active sound quality control systems were investigated. The simplified structure had less computational load, and the computational load of the modified structure was slightly increased compared to the traditional structure. Meanwhile, the two modified structures could remove the output signals of the feedforward control structure from the composition of the reference input signal. The influences of the feedback control filter and the line-spectrum noise cancellation control filter on the feedforward control filer were reduced, and the iteration processes of weight coefficients were more stable for the feedforward and feedback control filters in the two modified structures. It was also shown that the two modified structures for hybrid active sound quality control systems had the ability to cancel Gaussian random noise and promote the sound quality. In addition, a simplified structure using a new leaky FxLMS algorithm in the feedback control filter was proposed. This new leaky FxLMS algorithm could further improve the performance of noise reduction in the simplified structure. At the same time, the new leaky FxLMS algorithm could also avoid the excessive output signal for the feedback control filter by updating the leakage factor in a timely manner.

Author Contributions: The author thanks the co-authors for their support and contributions to this work. S.L. conceptualized the work and wrote the original draft of the work; X.L. provided help with the new leaky FxLMS algorithm; G.J. and T.Y. were the thesis supervisors and provided constructive suggestions and guidance for the work. All authors have read and agreed to the published version of the manuscript.

Funding: This research was funded by the National Natural Science Foundation of China, Grant Numbers [51822902, 51709066, and 51775125] and the Fundamental Research Funds for the Central Universities of China, Grant Nos. [HEUCFM180303 and HEUCF180305]. And the APC was funded by [51822902].

Acknowledgments: The authors gratefully acknowledge the financial support from the National Natural Science Foundation of China and the Fundamental Research Funds for the Central Universities of China.

Conflicts of Interest: The authors declare no conflicts of interest.

References

1. Kuo, S.M.; Morgan, D.R. *Active Noise Control Systems: Algorithms and DSP Implementations*, 1st ed.; John Wiley and Sons: New York, NY, USA, 1996.
2. Elliott, S.J. Active noise control. *IEEE Signal Process. Mag.* **1993**, *10*, 12–35. [CrossRef]
3. Miyazaki, N.; Kajikawa, Y. Head-mounted active noise control system with virtual sensing technique. *J. Sound Vib.* **2015**, *339*, 65–83. [CrossRef]
4. Gonzalez, A.; Ferrer, M.; Diego, M.D.; Pinero, G.; Garcia-Bonito, J.J. Sound quality of low-frequency and car engine noises after active noise control. *J. Sound Vib.* **2003**, *265*, 663–679. [CrossRef]
5. Zhong, J.; Tao, J.; Qiu, X. Increasing the performance of active noise control systems on ground with a finite size vertical reflecting surface. *Appl. Acoust.* **2019**, *154*, 193–200. [CrossRef]
6. Tao, J.; Wang, S.; Qiu, X. Performance of a multichannel active sound radiation control system near a reflecting surface. *Appl. Acoust.* **2017**, *123*, 1–8. [CrossRef]
7. Kuo, S.M.; Mallu, S. Adaptive active sound quality control algorithm. In Proceedings of the 2005 International Symposium on Intelligent Signal Processing and Communication Systems, Hong Kong, China, 13–16 December 2005; IEEE: Piscataway, NJ, USA, 2006.
8. Kuo, S.M.; Ji, M.J. Development and analysis of an adaptive noise equalizer. *IEEE Trans. Speech Audio Process.* **1995**, *3*, 217–222. [CrossRef]
9. Kuo, S.M.; Yang, Y. Broadband adaptive noise equalizer. *IEEE Signal Proc. Lett.* **1996**, *3*, 234–235. [CrossRef]
10. Liu, F.; Dong, M.; Wang, Y.; Yang, J.; Gu, L. Hybrid active sound quality control algorithm for vehicle interior noise. In Proceedings of the 46th Inter-Noise, Hong Kong, China, 27–30 August 2017.
11. Liu, F.; Mills, J.K.; Dong, M.; Gu, L. Active broadband sound quality control algorithm with accurate predefined sound pressure level. *Appl. Acoust.* **2017**, *119*, 78–87. [CrossRef]
12. Wang, Y.; Feng, T.; Wang, X.; Guo, H.; Qi, H. An improved LMS algorithm for active sound-quality control of vehicle interior noise based on auditory masking effect. *Mech. Syst. Signal Process.* **2018**, *108*, 292–303. [CrossRef]
13. Feng, J.; Gan, W.S. A broadband self-tuning active noise equalizer. *Signal Process.* **1997**, *62*, 251–256. [CrossRef]
14. Oliveira, L.P.R.D.; Stallaert, B.; Janssens, K.; Auweraer, H.V.D.; Sas, P.; Desmet, W. NEX-LMS: A novel adaptive control scheme for harmonic sound quality control. *Mech. Syst. Signal Process.* **2010**, *24*, 1727–1738. [CrossRef]
15. Wu, L.; Qiu, X.; Burnett, I.S.; Guo, Y. Decoupling feedforward and feedback structures in hybrid active noise control systems for uncorrelated narrowband disturbances. *J. Sound Vib.* **2015**, *350*, 1–10. [CrossRef]
16. Elliott, S. *Signal Processing for Active Control*; Elsevier: Amsterdam, The Netherlands, 2001; pp. 489–506.
17. Wang, T.; Gan, W.S. Stochastic analysis of FXLMS-based internal model control feedback active noise control systems. *Signal Process.* **2014**, *101*, 121–133. [CrossRef]
18. Zhang, L.; Tao, J.; Qiu, X. Performance analysis of decentralized multi-channel feedback systems for active noise control in free space. *Appl. Acoust.* **2013**, *74*, 181–188. [CrossRef]

19. Wu, L.; Qiu, X.; Guo, Y. A simplified adaptive feedback active noise control system. *Appl. Acoust.* **2014**, *81*, 40–46. [CrossRef]
20. Akhtar, M.T.; Mitsuhashi, W. Improving performance of hybrid active noise control systems for uncorrelated narrow band disturbances. *IEEE Trans. Audio Speech* **2011**, *19*, 2058–2066. [CrossRef]
21. Kajikawa, Y.; Gan, W.S.; Kuo, S.M. Recent advances on active noise control: Open issues and innovative applications. *APSIPA Trans. Signal Inf. Process.* **2012**, *1*, e3. [CrossRef]
22. Duan, J.; Li, M.; Lim, T.C.; Lee, M.R.; Cheng, M.T.; Vanhaaften, W.; Abe, T. Combined feedforward-feedback active control of road noise inside a vehicle cabin. *J. Vib. Acoust.* **2014**, *136*, 1–8. [CrossRef]
23. Padhi, T.; Chandra, M.; Kar, A.; Swamy, M.N.S. Design and analysis of an improved hybrid active noise control system. *Appl. Acoust.* **2017**, *127*, 260–269. [CrossRef]
24. Orlando, J.T.; Seara, R. Leaky-FxLMS algorithm: Stochastic analysis for Gaussian data and secondary path modeling error. *IEEE Trans. Speech Audio Process.* **2005**, *13*, 1217–1230.
25. Wu, L.; Qiu, X.; Guo, Y. A generalized leaky FxLMS algorithm for tuning the waterbed effect of feedback active noise control systems. *Mech. Syst. Signal Process.* **2018**, *106*, 13–23. [CrossRef]
26. Shi, D.Y.; Gan, W.S.; Lam, B. Two-gradient direction FXLMS: An adaptive active noise control algorithm with output constraint. *Mech. Syst. Signal Process.* **2019**, *116*, 651–667. [CrossRef]
27. Huang, J.; Zhang, B. The realization of adaptive 2-D FIR filter using constrained anti-Hebbian algorithm. *Microcomput. Inf.* **2006**, *22*, 304–306. (In Chinese)
28. Yang, T.; Zhu, L.; Li, X.; Pang, L. An online secondary path modeling method with regularized step size and self-tuning power scheduling. *J. Acoust. Soc. Am.* **2018**, *143*, 1076–1084. [CrossRef] [PubMed]
29. Steeneken, H. Personal active noise reduction with integrated speech communication devices: Development and assessment. *Noise Health* **1998**, *1*, 64–75.
30. Zhao, M.; Zhou, H.; Chen, G.; Zhu, B. *Mechanical Vibration and Noise*, 1st ed.; Science Press: Beijing, China, 2004.